

## New biostratigraphic and chemostratigraphic data from the Chicotte Formation (Llandoverly, Anticosti Island, Laurentia) compared with the Viki core (Estonia, Baltica)

Axel Munnecke<sup>a</sup> and Peep Männik<sup>b</sup>

<sup>a</sup> GeoZentrum Nordbayern, Fachgruppe Paläoumwelt, Loewenichstr. 28, D-91054 Erlangen, Germany; axel.munnecke@gzn.uni-erlangen.de

<sup>b</sup> Institute of Geology, Tallinn University of Technology, Ehitajate tee 5, 19086 Tallinn, Estonia; mannik@gi.ee

Received 6 March 2009, accepted 26 May 2009

**Abstract.** Due to the lack of biostratigraphically useful graptolites in the crinoidal and reefal Chicotte Formation on Anticosti Island (Québec, Canada), the precise chronostratigraphic position of the formation is not known. New stable carbon isotope and conodont data and a comparison with the detailed conodont distribution and  $\delta^{13}\text{C}$  development in the Viki core (Estonia) suggest an early Telychian age (*Pterospirifer eopennatus* to *P. a. angulatus* zones) for at least the lower half of the formation. This interval is characterized by a small but distinct positive excursion in  $\delta^{13}\text{C}$ , with peak values of +3.2‰ and +2.8‰ VPDB in the lowermost 10–15 m of the Chicotte Formation on Anticosti and in the Viki core, respectively.

**Key words:** conodonts, stable carbon isotopes, Anticosti, Estonia, Llandoverly, Telychian.

### INTRODUCTION

Anticosti Island, more than 200 km in length, is located in the Gulf of St Lawrence in eastern Canada (Fig. 1). The rocks exposed on the island are largely unaffected by tectonic stress and are extremely well preserved (Lespérance 1981a, 1981b; Petryk 1981; Copper & Long 1998; Chatterton et al. 2008). The succession on Anticosti consists of approximately 1 km thick, undeformed, fossiliferous limestones, shales, and minor siliciclastics, ranging in age from the Late Ordovician (Katian) to early Silurian (Telychian). The sediments accumulated in a slowly subsiding basin in a tropical setting south of the equator, along the NW margin of the Iapetus Ocean (Petryk 1981; Barnes 1988, 1989; MacNiocall et al. 1997; Copper & Long 1998; van Staal et al. 1998; Long 2007). The strata strike WNW–ESE (Fig. 1), with an average dip of less than 2° in a SW direction.

The sequence on Anticosti, with its excellent coastal-cliff and river-valley outcrops, represents one of the best-preserved exposures of shallow-water carbonates across the Ordovician–Silurian boundary (Petryk 1981; Barnes 1988). Most of the Llandoverly strata were formed below the storm wave base, except the Chicotte Formation (Fm.) and other reefal or shallow-water units (Brunton & Copper 1994). The youngest rocks on Anticosti are represented by the 80–90 m thick Chicotte Fm.

consisting of crinoidal limestones interpreted as inner-ramp shoal deposits, with reefs at three levels (Brunton & Copper 1994; Desrochers 2006). Due to the lack of biostratigraphically useful graptolites, the precise chronostratigraphic position of the Chicotte Fm. is still problematic. Whereas in some early papers at least the upper part of the formation was tentatively attributed to the lowermost Wenlock, today the consensus is that the entire formation is Telychian in age (e.g. Zhang & Barnes 2002; Desrochers 2006; Li & Copper 2006; Holland & Copper 2008).

A rough, preliminary set of stable isotope data from Llandoverly brachiopods of Anticosti Island has been published by Azmy et al. (1998). Unfortunately, their data do not include precise information from where the samples have been collected, and therefore a reliable location of some samples in the stratigraphic sequence is difficult. In general, the  $\delta^{13}\text{C}$  values do not show much variation, scattering around +1‰. An increase is observed from ca +0.5‰ in the upper part of the Jupiter Fm. (Ferrum and Pavillon members) to about 1.5‰ in the overlying Chicotte Fm.

The first data on conodonts of Anticosti Island (a brief note) were published in Sweet et al. (1971). In 1975 a programme was initiated by C. R. Barnes to study conodonts from Anticosti, and the exposed strata (including the Chicotte Fm.) were sampled at roughly 2 m intervals along the main sections along the Jupiter

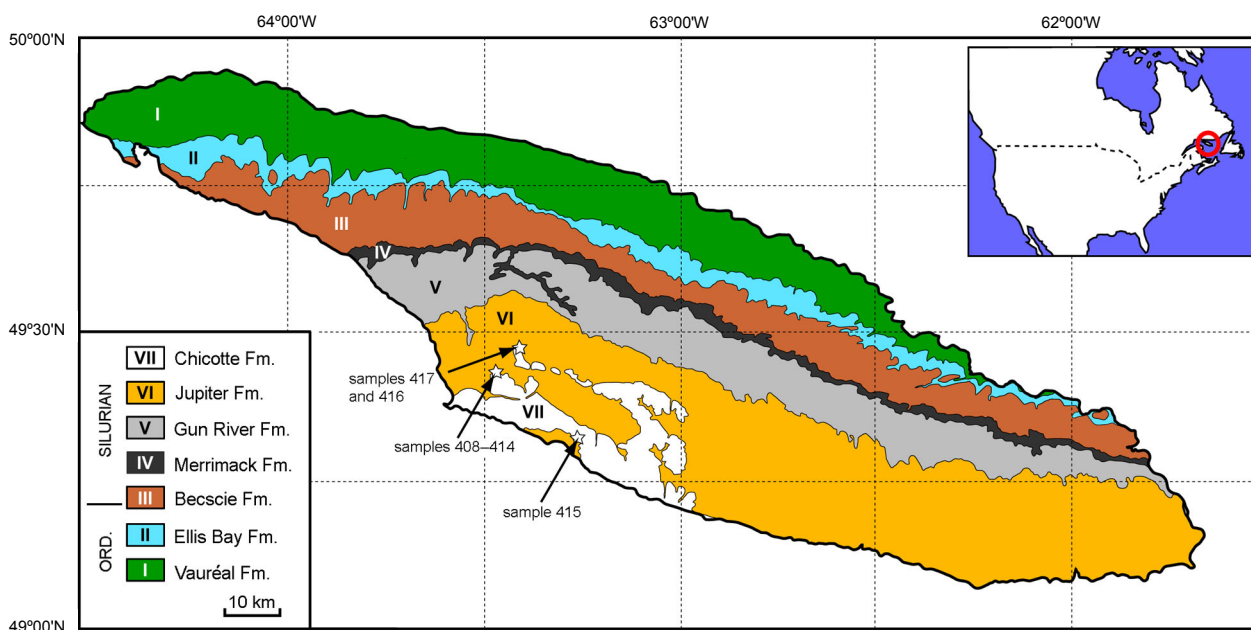


**Fig. 1.** Geological map of Anticosti Island (modified after Jin & Copper 1998 and Desrochers & Gauthier 2009), and the position of sampled localities.

and Salmon rivers and a few coastal bluffs (details in Barnes et al. 1981). The sampling of the Chicotte Fm. was limited to a few road-accessible sections in the lower part of the formation (Uyeno & Barnes 1983). The last authors assigned six samples from the sections at Pointe du Sud-Ouest and Brisants Jumpers, in the lowest 21 m of the Chicotte Fm., to the *Icriodella inconstans* Assemblage Zone. Additionally, a sample from a drill hole located north of The Jumpers (Uyeno & Barnes 1983, fig. 1: loc. C-89848) was studied. According to Uyeno & Barnes (1983, p. 7), this sample came from a level of about 24 m above the base of the Chicotte Fm. and is the only one yielding *Pterospathodus amorphognathoides amorphognathoides* Walliser, the nominal taxon of the *P. a. amorphognathoides* Zone.

In this study we present new conodont and stable carbon isotope data from four localities in the upper part of the Jupiter Fm. and the lower part of the Chicotte Fm. These data are compared with the detailed conodont biostratigraphy and with partly new  $\delta^{13}\text{C}$  information from the Viki core in western Saaremaa, Estonia (Fig. 2).

## MATERIAL AND METHODS

For the present study samples from four localities on Anticosti Island (Fig. 1) were investigated for stable carbon isotope geochemistry (studied from brachiopod

shells) and for conodonts. The GPS positions of the localities as well as the Geological Survey of Canada (GSC) numbers are summarized in Table 1. In total, 19 brachiopod shells and 7 micritic samples from a reef outcrop were measured for stable isotopes. The brachiopod samples were treated according to the procedure described in Samtleben et al. (2001). Additionally, 27 micritic samples from the Viki core, from the interval between 174.7 and 185.6 m, were investigated. A pilot study carried out by ourselves indicated that this interval correlates with the interval sampled on Anticosti Island. In the Viki core, samples V-1 to V-8 come from the upper Rumba Fm. and the others from the lower Velise Fm. (Table 2).

Homogeneous micritic material, drilled from cleaned, cut rock samples with a dentist's drill, was used in isotope studies of rock samples. Carbonate powders were reacted with 100% phosphoric acid (density >1.9, Wachter & Hayes 1985) at 75°C using a Kiel III online carbonate preparation line connected to a ThermoFinnigan 252 mass spectrometer. All values are reported in per mil relative to VPDB by assigning a  $\delta^{13}\text{C}$  value of +1.95‰ and a  $\delta^{18}\text{O}$  value of -2.20‰ to NBS19. Reproducibility was checked by replicate analysis of laboratory standards and it was better than  $\pm 0.04\%$  (1 $\sigma$ ). For the chemostratigraphic correlation presented here, only the  $\delta^{13}\text{C}$  values were used. The complete data set including  $\delta^{18}\text{O}$  values is given in Tables 1 and 2.

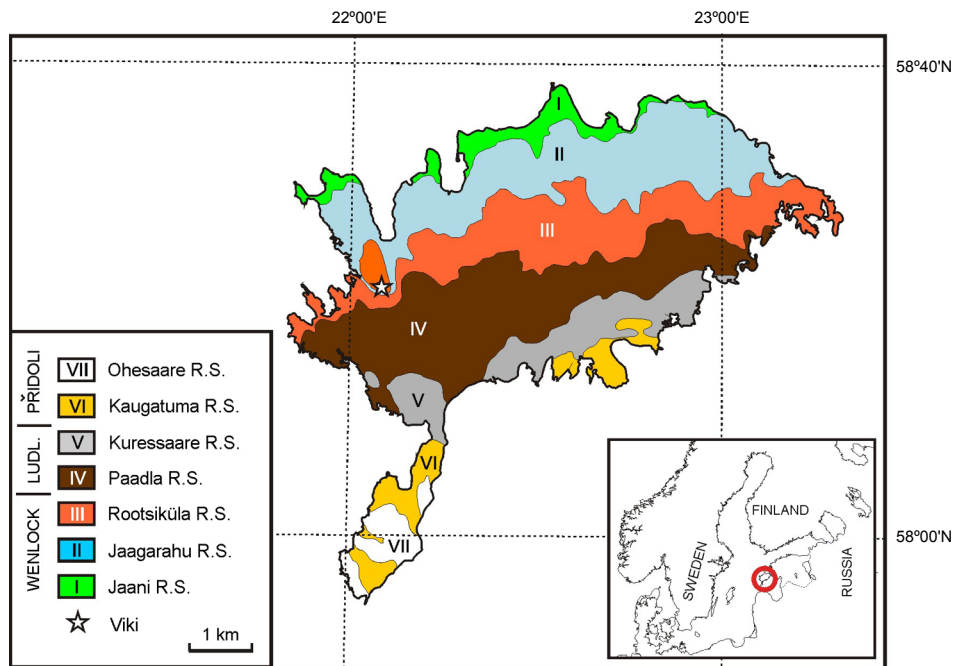


**Fig. 2.** The position of the Viki core and distribution of Silurian sediments. R.S., Regional Stage.

**Table 1.** Stable isotope values from Anticosti

Sample number	GSC number	GPS coordinates	Formation	Brachiopod genus	$\delta^{13}\text{C}$	$\delta^{18}\text{O}$
415-1	A1522	NTS 12/E 6 0481013, 5464119	Chicotte Fm.	<i>Stegerhynchus</i>	1.30	-5.67
415-2	A1522	NTS 12/E 6 0481013, 5464119	Chicotte Fm.	<i>Stegerhynchus</i>	1.11	-5.58
415-3	A1522	NTS 12/E 6 0481013, 5464119	Chicotte Fm.	<i>Stegerhynchus</i>	1.18	-5.56
415-4	A1522	NTS 12/E 6 0481013, 5464119	Chicotte Fm.	<i>Gotatrypa</i>	1.53	-5.65
415-5	A1522	NTS 12/E 6 0481013, 5464119	Chicotte Fm.	<i>Stegerhynchus</i>	1.17	-5.37
415-6	A1522	NTS 12/E 6 0481013, 5464119	Chicotte Fm.	? <i>Stegerhynchus</i>	1.22	-5.76
415-7	A1522	NTS 12/E 6 0481013, 5464119	Chicotte Fm.	? <i>Stegerhynchus</i>	1.37	-5.39
415-8	A1522	NTS 12/E 6 0481013, 5464119	Chicotte Fm.	<i>Stegerhynchus</i>	1.64	-5.49
415-9	A1522	NTS 12/E 6 0481013, 5464119	Chicotte Fm.	Undetermined	1.68	-5.74
408-1	A1562	NTS 12/E 6 0465959, 5468855	Chicotte Fm.	Micrite	2.64	-4.88
409-1	A1562	NTS 12/E 6 0465959, 5468855	Chicotte Fm.	Micrite	2.61	-5.46
410-1	A1562	NTS 12/E 6 0465959, 5468855	Chicotte Fm.	Micrite	2.72	-5.08
411-1	A1562	NTS 12/E 6 0465959, 5468855	Chicotte Fm.	Micrite	2.72	-5.02
412-1	A1562	NTS 12/E 6 0465959, 5468855	Chicotte Fm.	Micrite	2.63	-5.21
413-1	A1562	NTS 12/E 6 0465959, 5468855	Chicotte Fm.	Micrite	2.69	-5.09
414-1	A1562	NTS 12/E 6 0465959, 5468855	Chicotte Fm.	Micrite	2.80	-4.79
417-1	A1561b	NTS 12/E 6 0470689, 5479464	Chicotte Fm.	<i>Coolinia</i>	2.30	-5.01
417-2	A1561b	NTS 12/E 6 0470689, 5479464	Chicotte Fm.	<i>Coolinia</i>	2.99	-5.20
417-3	A1561b	NTS 12/E 6 0470689, 5479464	Chicotte Fm.	<i>Flabellitisia</i>	3.12	-5.33
417-4	A1561b	NTS 12/E 6 0470689, 5479464	Chicotte Fm.	<i>Flabellitisia</i>	3.15	-5.14
417-5	A1561b	NTS 12/E 6 0470689, 5479464	Chicotte Fm.	<i>Flabellitisia</i>	2.38	-5.76
416-1	A1561a	NTS 12/E 6 0470534, 5479315	Jupiter Fm.	<i>Gotatrypa</i>	1.07	-4.89
416-2	A1561a	NTS 12/E 6 0470534, 5479315	Jupiter Fm.	<i>Gotatrypa</i>	1.09	-4.81
416-4	A1561a	NTS 12/E 6 0470534, 5479315	Jupiter Fm.	<i>Gotatrypa</i>	0.57	-4.73
416-5	A1561a	NTS 12/E 6 0470534, 5479315	Jupiter Fm.	<i>Gotatrypa</i>	1.26	-4.42
416-6	A1561a	NTS 12/E 6 0470534, 5479315	Jupiter Fm.	<i>Gotatrypa</i>	1.08	-4.64

**Table 2.** Stable isotope data of the Viki core (‘–’ indicates samples where carbonate content was too low for isotope analysis)

Sample number	Level, m	Formation	Regional stage	Conodont stratigraphy	Occurrence of reddish colour	$\delta^{13}\text{C}$	$\delta^{18}\text{O}$
V-35	173.70	Velise	Adavere	Upper <i>P. eopennatus</i> ssp. n. 2	No	–	–
V-34	174.00	Velise	Adavere	Upper <i>P. eopennatus</i> ssp. n. 2	No	–	–
V-33	174.35	Velise	Adavere	Upper <i>P. eopennatus</i> ssp. n. 2	No	–	–
V-32	174.70	Velise	Adavere	Upper <i>P. eopennatus</i> ssp. n. 2	No	1.90	–5.48
V-31	175.05	Velise	Adavere	Upper <i>P. eopennatus</i> ssp. n. 2	Yes	–	–
V-30	175.45	Velise	Adavere	Upper <i>P. eopennatus</i> ssp. n. 2	No	2.19	–5.58
V-29	175.65	Velise	Adavere	Upper <i>P. eopennatus</i> ssp. n. 2	Yes	2.26	–5.61
V-28	176.15	Velise	Adavere	Upper <i>P. eopennatus</i> ssp. n. 2	No	–	–
V-27b	176.40	Velise	Adavere	Upper <i>P. eopennatus</i> ssp. n. 2	Yes	2.02	–4.61
V-27a	176.40	Velise	Adavere	Upper <i>P. eopennatus</i> ssp. n. 2	No	1.86	–4.54
V-26	176.90	Velise	Adavere	Upper <i>P. eopennatus</i> ssp. n. 2	Yes	–	–
V-25	177.20	Velise	Adavere	Lower <i>P. eopennatus</i> ssp. n. 2	No	–	–
V-24b	177.70	Velise	Adavere	Lower <i>P. eopennatus</i> ssp. n. 2	Yes	2.14	–4.43
V-24a	177.70	Velise	Adavere	Lower <i>P. eopennatus</i> ssp. n. 2	No	1.75	–4.32
V-23	178.00	Velise	Adavere	Lower <i>P. eopennatus</i> ssp. n. 2	Yes	2.11	–5.17
V-22	178.40	Velise	Adavere	Lower <i>P. eopennatus</i> ssp. n. 2	Yes	–	–
V-21	178.75	Velise	Adavere	Lower <i>P. eopennatus</i> ssp. n. 2	No	–	–
V-20	179.10	Velise	Adavere	Lower <i>P. eopennatus</i> ssp. n. 2	Yes	–	–
V-19b	179.35	Velise	Adavere	Lower <i>P. eopennatus</i> ssp. n. 2	No	2.29	–4.91
V-19a	179.35	Velise	Adavere	Lower <i>P. eopennatus</i> ssp. n. 2	No	2.79	–5.32
V-18	179.75	Velise	Adavere	Lower <i>P. eopennatus</i> ssp. n. 2	No	2.84	–5.44
V-17	180.15	Velise	Adavere	Lower <i>P. eopennatus</i> ssp. n. 2	No	2.67	–5.50
V-16	180.55	Velise	Adavere	Lower <i>P. eopennatus</i> ssp. n. 2	Yes	2.48	–5.35
V-15	180.90	Velise	Adavere	Lower <i>P. eopennatus</i> ssp. n. 2	Yes	2.52	–5.51
V-14	181.30	Velise	Adavere	<i>P. eopennatus</i> ssp. n. 1	Yes	2.23	–5.81
V-13	181.70	Velise	Adavere	<i>P. eopennatus</i> ssp. n. 1	Yes	2.14	–4.06
V-12	182.10	Velise	Adavere	<i>P. eopennatus</i> ssp. n. 1	Yes	–	–
V-11	182.50	Velise	Adavere	<i>P. eopennatus</i> ssp. n. 1	Yes	2.13	–3.58
V-10	183.00	Velise	Adavere	<i>P. eopennatus</i> ssp. n. 1	Yes	–	–
V-9b	183.30	Velise	Adavere	<i>P. eopennatus</i> ssp. n. 1	Yes	–	–
V-9a	183.30	Velise	Adavere	<i>P. eopennatus</i> ssp. n. 1	No	–	–
V-8	183.60	Rumba	Adavere	<i>P. eopennatus</i> ssp. n. 1	No	1.74	–5.35
V-7b	183.80	Rumba	Adavere	<i>P. eopennatus</i> ssp. n. 1	No	1.37	–5.58
V-7a	183.80	Rumba	Adavere	<i>P. eopennatus</i> ssp. n. 1	No	1.78	–5.36
V-6	184.10	Rumba	Adavere	<i>P. eopennatus</i> ssp. n. 1	No	1.84	–4.49
V-5	184.35	Rumba	Adavere	<i>D. staurognathoides</i>	No	1.50	–5.31
V-4b	184.60	Rumba	Adavere	<i>D. staurognathoides</i>	No	1.49	–5.09
V-4a	184.60	Rumba	Adavere	<i>D. staurognathoides</i>	No	1.35	–5.16
V-3	184.95	Rumba	Adavere	<i>D. staurognathoides</i>	No	1.25	–5.32
V-2	185.35	Rumba	Adavere	<i>D. staurognathoides</i>	No	0.28	–5.01
V-1	185.60	Rumba	Adavere	<i>D. staurognathoides</i>	No	0.35	–4.95

Traditional methods were used for processing the conodont samples. After dissolving a sample in 7–8% acetic acid, the residue was treated with 10% buffered formic acid to get rid of dolomite grains. The buffering of formic acid is essential to avoid damage to conodonts (Jeppsson & Anehus 1995). Final residues were small enough to be picked directly, without additional treatment with heavy liquid. All figured specimens of conodonts are deposited in collection GIT 583 in the Institute of Geology at Tallinn University of Technology, Estonia.

**RESULTS**

**Stable isotopes**

The mean  $\delta^{13}\text{C}$  values from Anticosti Island show a rapid increase from about 1.0‰ in the uppermost Jupiter Fm. (upper part of the Pavillon Member, locality A1561a, sample No. 416) to 2.8‰ in the lower part of the Chicotte Fm. (localities A1561b, A1562; samples 408–414 and 417; Fig. 3), with peak values of >3.1‰ (Table 1). In the youngest sample (locality A1522;

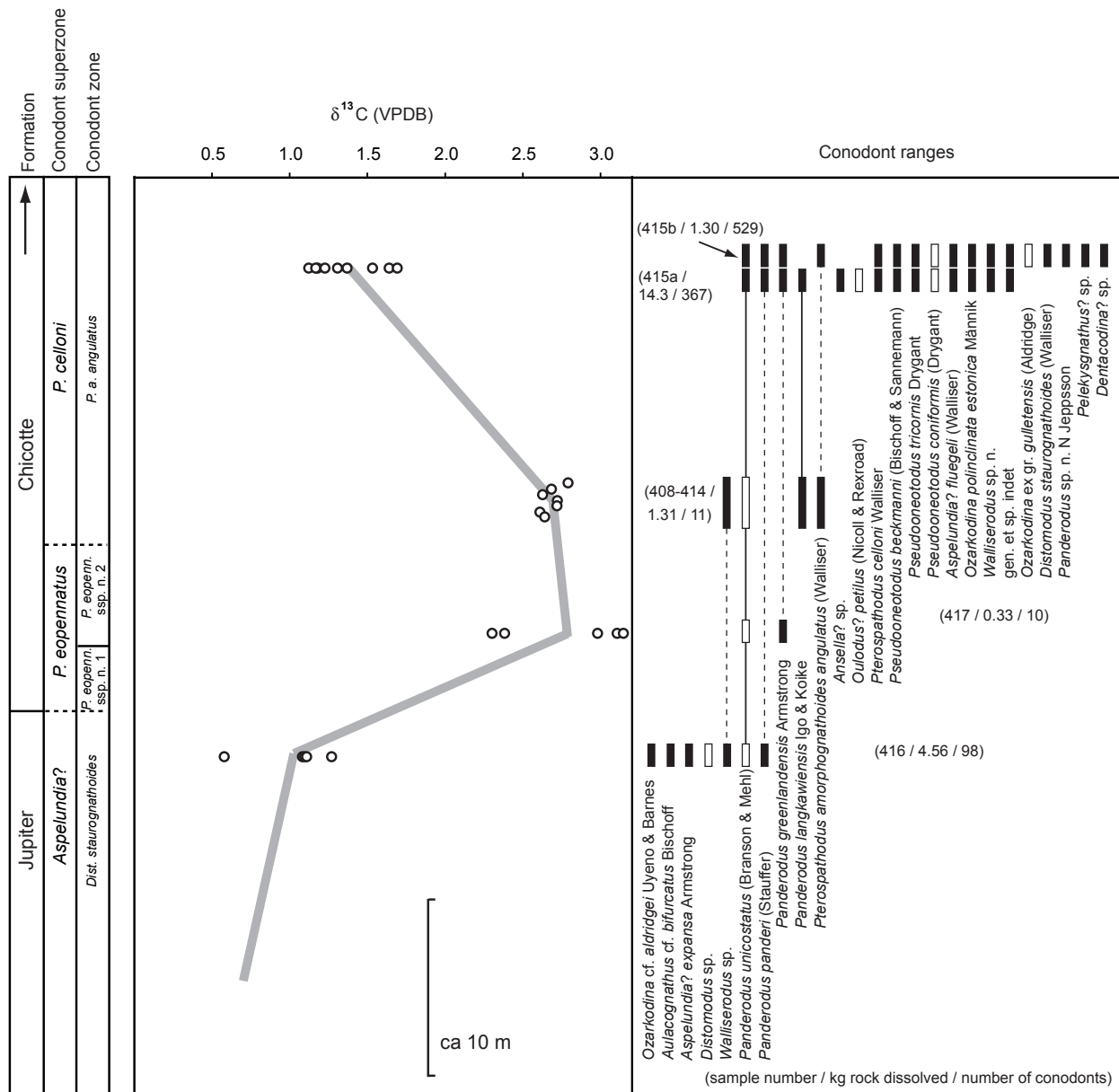


**Fig. 3.** Stable carbon isotope data from the uppermost Jupiter Formation and the Chicotte Formation and distribution of conodont taxa (solid line – continuous occurrence of a taxon; dotted line – sporadic occurrence of a taxon; filled box – reliable identification of a taxon; unfilled box – problematic identification of a taxon), zones and superzones in the Baltic region.

sample No. 415) investigated the values decrease again to around 1.4‰.

In the studied interval of the Viki core the rocks consist of argillaceous limestones, marlstones, and claystones. The claystones did not yield enough carbonate for stable isotope analysis. The  $\delta^{13}\text{C}$  values increase from ca +0.1‰ in the lower Rumba Fm. (?uppermost Aeronian) up to values between +2.0 and +3.0‰ in the interval spanning the uppermost part of the *P. eopennatus* ssp. n. 1 Zone to the lower part of the Upper *P. eopennatus* ssp. n. 2 Subzone (lower Velise Fm.; Fig. 4). Towards the top of the *P. eopennatus* ssp. n. 2 Zone the values of  $\delta^{13}\text{C}$  decrease gradually and remain more or less constant around +2.0‰ in the lower part of

the succeeding *P. a. angulatus* Zone (Fig. 4). Higher up in the core these values decrease continuously to about 1.3‰ in the *P. a. amorphognathoides* Zone (Kaljo et al. 2003). This means that a small positive  $\delta^{13}\text{C}$  excursion is observed in the *P. eopennatus* Superzone (lower Telychian) in the Viki core. It is interesting to note that the isotope excursion correlates with an interval where the otherwise greenish-grey rocks are frequently intercalated by red-coloured limestones, marls, and claystones (between 175 m and 183.5 m), whereas lower no such colour has been observed (Fig. 4; Table 2). Few thin red layers are present up to 153.8 m. In the Velise Fm. red strata form a continuous belt parallel to the shelf edge in the outer shelf region (Jeppsson & Männik 1993).

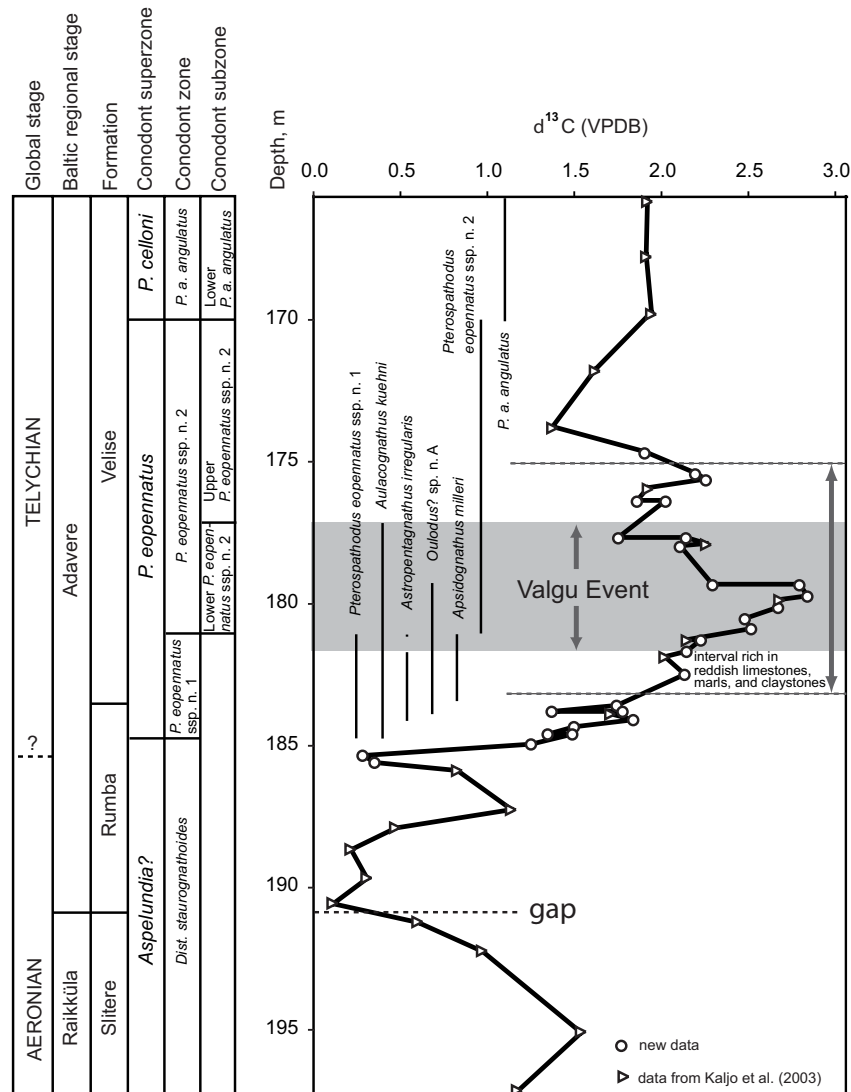


**Fig. 4.** Stratigraphy, stable carbon isotope data (from Kaljo et al. 2003 and new data), and ranges of selected conodont species (after Männik 2007a) in the Viki core. The position of the gap at the base of the Rumba Formation, which was positioned slightly higher in Kaljo et al. (2003), has been corrected based on new results.

## Conodonts

All samples yielded conodonts. The number of specimens per sample was highly variable, due to differences in sample size (from 0.33 to 14.3 kg) and in facies (Fig. 3). In total, 1068 identifiable conodont specimens were found (Figs 3, 5). The preservation of conodont specimens is good, with a conodont colour alteration index CAI = 1. In all samples, particularly in 416 and 417, the faunas are dominated by *Panderodus*. In sample 415 *Walliserodus* and *Pterospathodus* are quite common. This sample provided the richest and most variable fauna and allows quite precise dating of the strata (see Discussion). Sample 415 consists of two different lithologies which were processed separately (indicated as 415a and 415b in Fig. 3).

## DISCUSSION

Our data show a small but distinct positive stable carbon isotope excursion in the lower Telychian both on Baltica and Laurentia. Stable isotope data from this time slice are rare, and to our knowledge this excursion has so far been reported only by Kaljo & Martma (2000). Conodont data confirm the contemporaneous nature of the isotope excursions from the two areas.

The lowermost sample (No. 416, locality A1561a) comes from the top of the Jupiter Fm. (from the Pavillon Member) and is dominated by specimens of *Panderodus*. Here also *Ozarkodina* cf. *aldridgei* Uyeno & Barnes (Fig. 5A) and *Aulacognathus* cf. *bifurcatus* Bischoff (Fig. 5B) occur, which indicate that this sample comes from the *O. aldridgei* Zone sensu Zhang & Barnes (2002). This interval was previously referred to as the *aldridgei* fauna of the *Distomodus staurogathoides* Zone (Uyeno & Barnes 1983). According to Zhang & Barnes (2002), the *O. aldridgei* Zone includes also the top of the Jupiter Fm., which, based on the occurrence of *Icriodella inconstans* here, Uyeno & Barnes (1983) assigned to the *I. inconstans* Assemblage Zone. Although no *Icriodella* was found above the upper boundary of the Jupiter Fm., they also correlated the lower Chicotte Fm., the interval below the level of appearance of *P. a. amorphognathoides*, with this zone. Zhang & Barnes (2002) discarded the *I. inconstans* Zone in their revised zonation and stated that the *O. aldridgei* Zone is overlain by the *P. celloni* Zone. It seems that Zhang & Barnes (2002) correlate the base of the *P. celloni* Zone on Anticosti tentatively with the boundary between the Jupiter and Chicotte fms. As *Pterospathodus* had not been found in the lowermost Chicotte Fm., they evidently used the appearance of *Astropentagnathus irregularis*

Mostler to define the base of their *P. celloni* Zone. This agrees with data from other regions where *A. irregularis* appears together with *P. eopennatus* ssp. n. 1 Männik, together with the oldest form in the Telychian *Pterospathodus* lineage (Männik 1998, 2007a, 2008). *Astropentagnathus irregularis* is known from the *P. eopennatus* ssp. n. 1 Zone only (Männik 2007a). Accordingly, it is evident that the lowermost sample from the Chicotte Fm. (sample C-92675 in Uyeno & Barnes 1983) comes from the *P. eopennatus* ssp. n. 1 Zone. As *O. aldridgei* is very rare in the eastern Baltic, the strata below the *P. eopennatus* ssp. n. 1 Zone are assigned to the *D. staurogathoides* Zone in this region (Männik 2007b; Fig. 3).

The next sample (417; locality A1561b) comes from the lowermost Chicotte Fm. It is the smallest sample in our collection and yielded only 10 conodonts, mainly *Panderodus* cf. *unicostatus* (Branson & Mehl) (Fig. 3). This fauna does not allow precise dating of the level. However, considering the high  $\delta^{13}\text{C}$  values from brachiopods of the same sample (2.8‰; Fig. 3), it is most probable that this sample comes from the *P. eopennatus* Superzone (possibly from the lowermost *P. eopennatus* ssp. n. 2 Zone; Fig. 3). The lowermost *P. eopennatus* ssp. n. 2 Zone is also indicated by the low number of conodont specimens in this sample: at the lower boundary of the zone the abundance of conodonts drops considerably (e.g. Männik 2005).

Sample 408–414 (locality A1562) is a composite one and includes seven small pieces of rock, all collected from a bryozoan mound but from different levels (distance between the lowermost and the uppermost sample is 5.5 m). Only 11 conodont specimens were found. Three of them definitely belong to *P. amorphognathoides*, probably to *P. a. angulatus* (Figs 3; 5J, K). *Panderodus langkawiensis* Igo & Koike (Fig. 5E) and poorly preserved specimens of *Panderodus* and *Walliserodus* are also found. This sample suggests the *P. a. angulatus* Zone, probably its lower part (see below; Fig. 3).

The highest sample (415; locality A1522) comes from the same conodont zone, about 25 m above the base of the Chicotte Fm. However, due to different lithologies (processed separately, indicated as 415a and 415b) the number of specimens in these subsamples differs considerably (Fig. 3). Subsample 415a consists of micritic reefal limestone, was 14.3 kg in weight, and yielded 367 conodont specimens. Subsample 415b comes from a bed of unsorted, mainly fine-grained bioclastic limestone in which complete brachiopod shells and big fragments of crinoid stems are common. The weight of 415b was 1.3 kg and it yielded 529 identifiable conodont specimens. Occurring in these samples, *P. celloni*

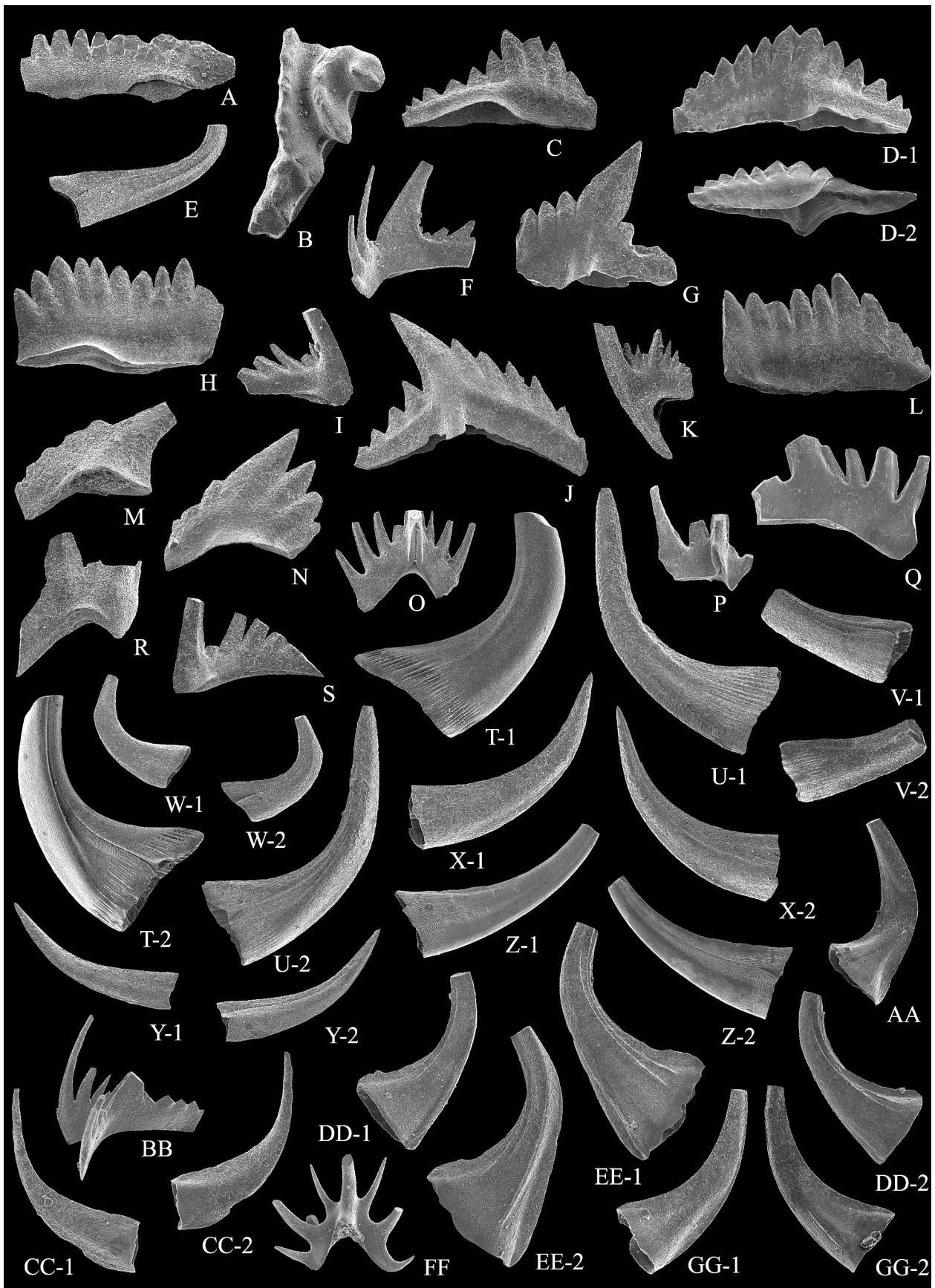
(Walliser) (Figs 3; 5C, D, G) indicates that these strata are older than the *P. a. amorphognathoides* Zone. *Ozarkodina polinclinata estonica* Männik (Fig. 5F, H, I) refers the samples to the lower and/or middle part of the *P. celloni* Superzone (to the *P. a. angulatus* or *P. a. lennarti* Zone). Although the elements of *P. amorphognathoides* in 415b are too poorly preserved to be properly identified, they look most similar to *P. a. angulatus* (Walliser) (Fig. 5L, N). Another indication of the *P. a. angulatus* Zone is the occurrence of *Pelekysgnathus?* sp. (Fig. 5M) in this sample. In Estonia *Pelekysgnathus?* sp. ranges from the upper *P. eopennatus* ssp. n. 2 Zone to the lower *P. a. angulatus* Zone (Männik 2007a). Also in the Cellon section *Pelekysgnathus?* sp. occurs together with *P. a. angulatus* (in sample 10D in O. H. Walliser's collection; pers. obs. by P. Männik). Other taxa most common in sample 415 include *Aspelundia? fluegeli* (Walliser) (Fig. 5O–S), *Pand. greenlandensis* Armstrong (Fig. 5T–W), *Pand. unicostatus* (Branson & Mehl) (Fig. 5X–Z), and *Walliserodus* sp. n. (Fig. 5AA, DD–EE, GG), which is morphologically quite similar to *Walliserodus* sp. n. b from Estonia (e.g. Männik 2008, figs 10K, L, N, Q–S).

In summary, the stratigraphic position of at least the lower part of the Chicotte Fm. ranges from the

*P. eopennatus* ssp. n. 1 Zone to the *P. a. angulatus* Zone. This time interval is characterized by significant changes in depositional environments, which resulted in extinctions in conodont fauna (Valgu Event, Männik 2005, 2007c; Fig. 4). The Valgu Event, as recognized in Estonia, started in the latest *P. eopennatus* ssp. n. 1 time (temporal disappearance of *Astropentagnathus irregularis*, = Datum 1 of the event) and ended in the middle of *P. eopennatus* ssp. n. 2 time (extinction of *Aulacognathus kuehni* Mostler, = Datum 6). Besides the extinctions of several taxa, changes in the environment also caused considerable decrease in the abundance of conodonts at the early stage of the event.

In the Viki core the interval spanning the isotope excursion (roughly 10 m thick) shows frequent intercalations of micritic limestones, marls, and claystones with reddish or brownish colours (Table 2). On Anticosti Island the 80–90 m thick Chicotte Fm. is built by pure crinoidal limestones and reefs. According to Ziegler & McKerrow (1975), reddish colour in sediments might be the result of (a) transgressive pulses, (b) high sedimentation rates, (c) quiet outer shelf and deeper marine conditions, or (d) availability of a suitably oxidized source area. At least (a) and (c), but probably also (b) agree with the red colours in the Viki core. Munnecke et al.

**Fig. 5.** Selected conodonts. **A**, *Ozarkodina* cf. *aldridgei* Uyeno & Barnes, GIT 583-1, lateral view of Pa element, sample 416,  $\times 70$ . **B**, *Aulacognathus* cf. *bifurcatus* Bischoff, GIT 583-2, upper view of a fragment of Pa element, sample 416,  $\times 50$ . **C, D, G**, *Pterospathodus celloni* (Walliser). **C**, GIT 583-3, inner lateral view of sinistral Pa element, sample 415b,  $\times 70$ ; **D**, GIT 583-4, inner lateral (D-1) and lower (D-2) views of dextral Pa element, sample 415a,  $\times 70$ ; **G**, GIT 583-5, outer lateral view of sinistral Pb<sub>1</sub> element, sample 415a,  $\times 70$ . **E**, *Panderodus langkawiensis* Igo & Koike, GIT 583-6, lateral view of high-based graciliform element, samples 408–414,  $\times 70$ . **F, H, I**, *Ozarkodina polinclinata estonica* Männik. **F**, GIT 583-7, inner lateral view of dextral Sc element, sample 415a,  $\times 70$ ; **H**, GIT 583-8, inner lateral view of sinistral Pa element, sample 415b,  $\times 70$ ; **I**, GIT 583-9, inner lateral view of sinistral M element, sample 415a,  $\times 70$ . **J–L, N**, *Pterospathodus amorphognathoides angulatus* (Walliser). **J**, GIT 583-10, outer lateral view of dextral Pb<sub>1</sub> element, samples 408–414,  $\times 70$ ; **K**, GIT 583-11, inner lateral view of dextral Sc<sub>2</sub> element, samples 408–414,  $\times 70$ ; **L**, GIT 583-12, lateral view of a fragment of Pa element, sample 415b,  $\times 70$ ; **N**, GIT 583-13, outer lateral view of sinistral Pb<sub>2</sub> element, sample 415b,  $\times 70$ . **M**, *Pelekysgnathus?* sp., GIT 583-14, outer lateral view of sinistral Pa element, sample 415b,  $\times 70$ . **O–S**, *Aspelundia? fluegeli* (Walliser). **O**, GIT 583-15, posterior view of Sa element, sample 415a,  $\times 70$ ; **P**, GIT 583-16, posterior view of dextral Sb element, sample 415a,  $\times 70$ ; **Q**, GIT 583-17, inner lateral view of sinistral Sc element, sample 415a,  $\times 70$ ; **R**, GIT 583-18, inner lateral view of sinistral Pa? element, sample 415b,  $\times 70$ ; **S**, GIT 583-19, inner lateral view of dextral M element, sample 415b,  $\times 70$ . **T–W**, *Panderodus greenlandensis* Armstrong. **T**, GIT 583-20, unfurrowed (T-1) and furrowed (T-2) faces of sinistral arcuatiform element, sample 415a,  $\times 40$ ; **U**, GIT 583-21, unfurrowed (U-1) and furrowed (U-2) faces of dextral falciform element, sample 415b,  $\times 40$ ; **V**, GIT 583-22, furrowed (V-1) and unfurrowed (V-2) faces of sinistral tortiform element, sample 415b,  $\times 40$ ; **W**, GIT 583-23, unfurrowed (W-1) and furrowed (W-2) faces of dextral truncatiform element, sample 415a,  $\times 50$ . **X–Z**, *Panderodus unicostatus* (Branson & Mehl). **X**, GIT 583-24, unfurrowed (X-1) and furrowed (X-2) faces of sinistral falciform element, sample 415a,  $\times 50$ ; **Y**, GIT 583-25, unfurrowed (Y-1) and furrowed (Y-2) faces of dextral tortiform element, sample 415a,  $\times 50$ ; **Z**, GIT 583-26, unfurrowed (Z-1) and furrowed (Z-2) faces of sinistral arcuatiform element, sample 415a,  $\times 50$ . **AA, DD, EE, GG**, *Walliserodus* sp. n. **AA**, GIT 583-27, inner lateral view of sinistral curvatiform element, sample 415a,  $\times 70$ ; **DD**, GIT 583-28, inner (DD-1) and outer (DD-2) lateral views of sinistral low-based deboltiform element, sample 415a,  $\times 70$ ; **EE**, GIT 583-29, outer (EE-1) and inner (EE-2) lateral views of sinistral multicostatiform element, sample 415a,  $\times 70$ ; **GG**, GIT 583-30, inner (GG-1) and outer (GG-2) lateral views of unicostatiform element, sample 415a,  $\times 70$ . **BB**, gen. et sp. indet., GIT 583-31, lateral view, sample 415a,  $\times 70$ . **CC**, *Ansella?* sp., GIT 583-32, outer (CC-1) and inner (CC-2) lateral views of sinistral asymmetrical acostate element, sample 415a,  $\times 100$ . **FF**, *Oulodus? petilus* (Nicoll & Rexroad), GIT 583-33, posterior view of dextral Sb element, sample 415a,  $\times 70$ .



(2003) have shown that the prominent  $\delta^{13}\text{C}$  excursions, at least from the late Ordovician to uppermost Silurian (including the Hirnantian excursion), exhibit lithological, geochemical, and palaeontological similarities, indicating common steering mechanisms. For example, these excursions are characterized by pure carbonates and abundant reefs in shallow-water settings, by oxygenated sediments in deep-shelf environments, and the onset of the excursion is usually correlated with conodont extinctions ('Events' of Jeppsson 1990; Munnecke et al. 2003). The causes of the isotope excursions are a matter of intense debate (e.g. Kaljo et al. 2003, 2008; Loydell 2007, 2008; Cramer & Munnecke 2008), and it is beyond the scope of the present paper to answer the question about the steering mechanisms. However, the comparatively small excursion in the lower Telychian reported here interestingly shows the same signatures as the excursions mentioned above, and therefore we assume that similar environmental changes are likely responsible.

**Acknowledgements.** The authors are especially grateful to Paul Copper for guidance in the field, identification of brachiopods, many fruitful discussions, and for considerably improving an early draft of the manuscript, as well as to Michael Joachimski, Marco Vecoli, and Richard Jänig for their help in the field. The study benefited from help provided by Lennart Jeppsson. We are grateful for constructive reviews by Bradley Douglas Cramer and André Desrochers. The study of A. Munnecke was funded by the Schmauser-Stiftung (Erlangen, Germany) and by the German Research Foundation (Mu 2352/1), and of P. Männik by the Estonian Science Foundation (grant No. 7138). This is a contribution to IGCP 503.

## REFERENCES

- Azmy, K., Veizer, J., Bassett, M. G. & Copper, P. 1998. Oxygen and carbon isotopic composition of Silurian brachiopods: implications for coeval seawater and glaciations. *GSA Bulletin*, **110**, 1499–1512.
- Barnes, C. R. 1988. Stratigraphy and paleontology of the Ordovician–Silurian boundary interval. In *A Global Analysis of the Ordovician–Silurian Boundary* (Cocks, L. M. R. & Rickards, R. B., eds), *Bulletin of the British Museum (Natural History), Geology*, **43**, 195–219.
- Barnes, C. R. 1989. Lower Silurian chronostratigraphy of Anticosti Island, Québec. In *A Global Analysis of the Ordovician–Silurian Boundary* (Holland, C. H. & Bassett, M. G., eds), *National Museum of Wales, Geology Series*, **9**, 101–108.
- Barnes, C. R., Petryk, A. A. & Bolton, T. E. 1981. Anticosti Island, Québec. In *Field Meeting, Anticosti-Gaspé, Québec, 1981, vol. I: Guidebook* (Lespérance, P. J., ed.), pp. 1–24. Subcommittee on Silurian Stratigraphy, Ordovician–Silurian Boundary Working Group, Université de Montréal.
- Brunton, F. R. & Copper, P. 1994. Paleoeologic, temporal, and spatial analysis of Early Silurian reefs of the Chicotte Formation, Anticosti Island, Quebec, Canada. *Facies*, **31**, 57–80.
- Chatterton, B. D. E., Copper, P., Dixon, O. A. & Gibb, S. 2008. Spicules in Silurian tabulate corals from Canada, and implications for their affinities. *Palaeontology*, **51**, 173–198.
- Copper, P. & Long, D. G. F. 1998. Sedimentology and paleontology of the Late Ordovician through Early Silurian shallow water carbonates and reefs of the Anticosti Island, Québec. In *Geological Association of Canada, Annual Meeting, Québec City, Field Trip B8 Guidebook*, pp. 55–94.
- Cramer, B. D. & Munnecke, A. 2008. Early Silurian  $\delta^{13}\text{C}$  excursions and their relationship to glaciations, sea-level changes and extinction events: Discussion. *Geological Journal*, **43**, 517–519.
- Desrochers, A. 2006. Rocky shoreline deposits in the Lower Silurian (upper Llandovery, Telychian) Chicotte Formation, Anticosti Island, Québec. *Canadian Journal of Earth Sciences*, **43**, 1205–1214.
- Desrochers, A. & Gauthier, É. L. 2009. *Carte géologique de l'île d'Anticosti (1/250 000)*. Ministère des Ressources naturelles de la faune du Québec, DV 2009-03.
- Holland, C. H. & Copper, P. 2008. Ordovician and Silurian nautiloid cephalopods from Anticosti Island: trajet across the Ordovician–Silurian (O–S) mass extinction boundary. *Canadian Journal of Earth Sciences*, **45**, 1015–1038.
- Jeppsson, L. 1990. An oceanic model for lithological and faunal changes tested on the Silurian record. *Journal of the Geological Society, London*, **147**, 663–674.
- Jeppsson, L. & Anehus, R. 1995. A buffered formic acid technique for conodont extraction. *Journal of Paleontology*, **69**, 790–794.
- Jeppsson, L. & Männik, P. 1993. High-resolution correlations between Gotland and Estonia near the base of the Wenlock. *Terra Nova*, **5**, 348–358.
- Jin, J. & Copper, P. 1998. *Kulumbella* and *Microcardinalia* (*Chiastodoca*) new subgenus, Early Silurian divaricate stricklandiid brachiopods from Anticosti Island, eastern Canada. *Journal of Paleontology*, **72**, 441–453.
- Kaljo, D. & Martma, T. 2000. Carbon isotopic composition of Llandovery rocks (East Baltic Silurian) with environmental interpretation. *Proceedings of Estonian Academy of Sciences, Geology*, **49**, 267–283.
- Kaljo, D., Martma, T., Männik, P. & Viira, V. 2003. Implications of Gondwana glaciations in the Baltic late Ordovician and Silurian and a carbon isotopic test of environmental cyclicity. *Bulletin de la Société Géologique de France*, **174**, 59–66.
- Kaljo, D., Hints, L., Männik, P. & Nölvak, J. 2008. The succession of Hirnantian events based on data from Baltica: brachiopods, chitinozoans, conodonts, and carbon isotopes. *Estonian Journal of Earth Sciences*, **57**, 197–218.
- Lespérance, P. J. (ed.) 1981a. *Field Meeting, Anticosti-Gaspé, Québec, 1981. IUGS Subcommittee on Silurian*

- Stratigraphy – Ordovician–Silurian Boundary Working Group. I Guidebook*. Département de Géologie, Université de Montréal, 56 pp.
- Lespérance, P. J. (ed.) 1981b. *Field Meeting, Anticosti-Gaspé, Québec, 1981. IUGS Subcommission on Silurian Stratigraphy – Ordovician–Silurian Boundary Working Group. II Stratigraphy and Paleontology*. Département de Géologie, Université de Montréal, 321 pp.
- Li, R. & Copper, P. 2006. Early Silurian (Llandovery) orthide brachiopods from Anticosti Island, eastern Canada: the O/S extinction recovery fauna. *Special Papers in Palaeontology*, **76**, 1–71.
- Long, D. G. F. 2007. Tempestite frequency curves: a key to Late Ordovician and Early Silurian subsidence, sea-level change, and orbital forcing in the Anticosti foreland basin, Quebec, Canada. *Canadian Journal of Earth Sciences*, **44**, 413–431.
- Loydell, D. K. 2007. Early Silurian positive  $\delta^{13}\text{C}$  excursions and their relationship to glaciations, sea-level changes and extinction events. *Geological Journal*, **42**, 531–546.
- Loydell, D. K. 2008. Early Silurian  $\delta^{13}\text{C}$  excursions and their relationship to glaciations, sea-level changes and extinction events: Reply. *Geological Journal*, **43**, 511–515.
- MacNiocall, C., van der Plum, B. A. & van der Voo, R. 1997. Ordovician paleogeography and the evolution of the Iapetus ocean. *Geology*, **25**, 159–162.
- Männik, P. 1998. Evolution and taxonomy of the Silurian conodont *Pterospirifer*. *Palaeontology*, **41**, 1001–1050.
- Männik, P. 2005. Early Telychian Valgu Event – some preliminary data from Estonia. In *Evolution of Life on the Earth: Proceedings of the III International Symposium* (Podobina, V. M., ed.), pp. 134–137. Tomsk State University, Tomsk.
- Männik, P. 2007a. An updated Telychian (Late Llandovery, Silurian) conodont zonation based on Baltic faunas. *Lethaia*, **40**, 45–60.
- Männik, P. 2007b. Upper Ordovician and lower Silurian conodont biostratigraphy in Estonia: general overview of recent developments. *Estonian Journal of Earth Sciences*, **56**, 35–46.
- Männik, P. 2007c. Some comments on the Telychian–Early Sheinwoodian conodont faunas, events and stratigraphy. *Acta Palaeontologica Sinica*, **46**, 305–310.
- Männik, P. 2008. Conodont dating of some Telychian (Silurian) sections in Estonia. *Estonian Journal of Earth Sciences*, **57**, 156–169.
- Munnecke, A., Samtleben, C. & Bickert, T. 2003. The Ireviken Event in the lower Silurian of Gotland, Sweden – relation to similar Palaeozoic and Proterozoic events. *Palaeogeography, Palaeoclimatology, Palaeoecology*, **195**, 99–124.
- Petryk, A. A. 1981. Stratigraphy, sedimentology, and palaeogeography of the Upper Ordovician–Lower Silurian of Anticosti Island, Québec. In *Stratigraphy and Paleontology. Field Meeting, Anticosti-Gaspé, Québec, 1981, Vol. II* (Lespérance, P. J., ed.), pp. 11–40. Département de Géologie, Université de Montréal.
- Samtleben, C., Munnecke, A., Bickert, T. & Pätzold, J. 2001. Shell succession, assemblage and species dependent effects on the C/O-isotope composition of brachiopods – examples from the Silurian of Gotland. *Chemical Geology*, **175**, 61–107.
- Sweet, W. C., Ethington, R. L. & Barnes, C. R. 1971. North American Middle and Upper Ordovician conodont faunas. *Geological Survey of America Memoir*, **127**, 163–193.
- Uyeno, T. T. & Barnes, C. R. 1983. Conodonts of the Jupiter and Chicotte formations (lower Silurian), Anticosti Island, Québec. *Geological Survey of Canada Bulletin*, **355**, 1–49.
- Van Staal, C. R., Dewey, J. F., MacNiocall, C. & McKerrow, W. S. 1998. The Cambrian–Silurian tectonic evolution of the northern Appalachians and British Caledonides: history of a complex, west and southwest Pacific-type segment of Iapetus. *Geological Society, London, Special Publications*, **143**, 199–242.
- Wachter, E. & Hayes, J. M. 1985. Exchange of oxygen isotopes in carbon-dioxide – phosphoric acid systems. *Chemical Geology*, **52**, 365–374.
- Zhang, S. & Barnes, C. R. 2002. A new Llandovery (early Silurian) conodont biozonation and conodonts from the Becscie, Merrimack, and Gun River formations, Anticosti Island, Québec. *Journal of Paleontology*, **76**, 1–46.
- Ziegler, A. M. & McKerrow, W. S. 1975. Silurian marine red beds. *American Journal of Science*, **275**, 31–56.

## Uusi võrdlevaid bio- ja kemostratigraafilisi andmeid Chicotte kihistust (Llandovery, Anticosti, Laurentia) ning Viki puursüdamikust (Eesti, Baltica)

Axel Munnecke ja Peep Männik

Anticosti saarel paljanduvate noorimate kihtide, Chicotte kihistu rifflubjakivide vanus on olnud pikka aega problemaatiline. Uued,  $\delta^{13}\text{C}$ -väärtustes toimuvate muutuste ja konodontide leviku võrdlevad uuringud Anticosti läbilõigetest ning Viki puursüdamikust Saaremaal näitavad, et Chicotte kihistu alumine pool on Vara-Telychi vanusega. Mõlemas regioonis iseloomustab seda intervalli selge lühiajaline  $\delta^{13}\text{C}$ -väärtuste oluline kasv.